Biochemical Investigation of Inhibitory Activities of Plant-Derived Bioactive Compounds Against Carbohydrate and Glucagon-Like Peptide-1 Metabolizing Enzymes

Muhammad Fiaz Khalid[1], Kanwal Rehman[2], Kanwal Irshad[1] ⓘ, Tahir Ali Chohan[3], and Muhammad Sajid Hamid Akash[1] ⓘ

Abstract

The aim of current study was to investigate the inhibitory activities of resveratrol and taxifolin against α-amylase, α-glucosidase, and DPP-IV enzymes *via in vitro* analysis which was further validated by *in silico* studies. The analysis of molecular docking was also done to determine the binding capabilities of resveratrol and taxifolin with α-amylase, α-glucosidase, and DPP-IV enzymes. Resveratrol and taxifolin having IC_{50} values, 47.93 ± 5.21 μM and 45.86 ± 3.78 μM, respectively, showed weaker effect than acarbose (4.6 ± 1.26 μM) on α-amylase but showed significant effect to inhibit α-glucosidase (32.23 ± .556 μM and 31.26 ± .556 μM, respectively). IC_{50} value of resveratrol and taxifolin (5.638 ± .0016 μM and 6.691 ± .004 μM) in comparison to diprotin A (IC_{50}: 7.21 ± .021 μM) showed that they have significant inhibitory effect on DPP-IV enzyme. Our results illustrated that resveratrol and taxifolin have potential to prevent the metabolism of carbohydrates *via* inhibition of α-amylase and α-glucosidase, and prolongs metabolic function of incretin by inhibiting the enzymatic activity of DPP-IV. The results of molecular docking have also revealed that resveratrol and taxifolin have significant affinity to bind with α-amylase, α-glucosidase, and DPP-IV in comparison with standard drugs such as acarbose, miglitol, and diprotin.

Introduction

Diabetes mellitus (DM) is a metabolic disorder which is characterized by hyperglycemic state for a prolonged period due to abnormal insulin secretion and function.[1] WHO (World Health Organization) has reported 3.2 million deaths due to DM.[2] The major risk factors for the occurrence of DM include life style, high intake of calories, genetic predisposition, and obesity.[3] For the treatment of DM, typically anti-diabetic drugs possessing different mechanism of action are known but these drugs have some serious side effects such as weight gain, nutritional disorders, hypoglycemia, allergic reactions, and liver damage.[4] These side effects have gained the attention of researchers to discover the novel anti-diabetic agents having less side effects. Present research leads to the development of therapeutic agents which have more than one therapeutic target to achieve the adequate level of blood glucose.[5]

[1] Department of Pharmaceutical Chemistry, Government College University, Faisalabad, Pakistan
[2] Department of Pharmacy, The Women University, Multan, Pakistan
[3] Institute of Pharmaceutical Sciences, University of Veterinary and Animal Sciences, Lahore, Pakistan

Corresponding Author:
Muhammad Sajid Hamid Akash, Department of Pharmaceutical Chemistry, Government College University, Faisalabad, Punjab 38000, Pakistan.
Email: sajidakash@gcuf.edu.pk

Carbohydrates are the main source of energy for animals and human beings which are digested by α-amylase which is a hydrolase that cleaves 1,4-glucosidic bond in the linear regions in starch, glycogen and in various other different types of disaccharides and oligosaccharides. The hydrolytic action accompanied by α-amylase converts complex carbohydrates into simple monosaccharide (glucose units).[6,7] Similarly, hypothalamus-pituitary-adrenal axis converts them into simple sugars and facilitates the absorption of monomers of sugars from intestine into the blood stream[7] that ultimately produces hyperglycemia and various other types of metabolic disorders.[8] The suppression of human α-amylase (HPA) and α-glucosidase (GLU) activities results in less availability of individual monomers of absorbable sugars which ultimately decreases the postprandial hyperglycemia.[8,9] It has been well-documented that plant-derived bioactive compounds may inhibit the enzymatic activity of HPA reversibly and competitively to maintain the glycemic status within the body.[7,10,11] In diabetic patients, incretin-based treatment proved helpful in decreasing the incidence of hyperglycemia.[12] Upon the uptake of nutrients, intestinal enteroendocrine cells release incretins and peptide hormones which stimulate the secretion of insulin.[13] It has been observed that incretin hormones such as glucose-dependent insulin-tropic (GIP) and polypeptide i.e., glucagon-like peptide-1 (GLP-1) are involved in stimulating the secretion of insulin depending upon the level of glucose in healthy individual. After the secretion of GLP-1 and GIP, they are transformed into inactive metabolites via cleavage of N-terminal alanine or praline.[14,15] The half-life of these hormones is about 2 minutes. They are rapidly degenerated by dipeptidyl peptidase IV (DPP-IV).[16] GLP-1 is regarded as the most important substrate of DPP-IV enzyme. The nutrient dependent secretion of GLP-1 can induce the release of insulin from β-cells of pancreatic islets in order to regulate the glycemic status of the body. However, DPP-IV rapidly degrades GLP-1 due to which it performs its action for a short period of time. Hence, DPP-IV inhibition increases the level of insulin in systemic circulation by inhibiting the degradation of GLP-1.[17] This phenomenon leads to decrease the elevated level of blood glucose. This is the most important therapeutic intervention and target that leads the researcher for the development of DPP-IV inhibitors in order to alleviate the glucose burden in blood.[18]

Resveratrol (RSV) is a polyphenolic compound belonging to a class of stilbenes and found in many food products and fruits.[19] RSV has a potential to reduce the oxidative stress, increases insulin sensitivity, and restores the insulin signaling pathway which ultimately improves the glucose metabolism.[20] The reduction in oxidative stress improves the insulin signaling pathway and enhances the insulin sensitivity.[21] RSV alters the expression of adipokines by inhibiting the inflammatory response and reduces the resistance of insulin via activation of sirtuins 1 (SIRT1), principal modulator of to regulate insulin sensitivity and glucose homeostasis.[22]

RSV ameliorates the glycemic status and blood glucose level in type 2 diabetic patients.[23] Thus, supplementation of RSV in diabetic patient improves the glycemic status, HbA1c level, cholesterol, and systolic pressure.[24] The literature showed that RSV has been used in the treatment of diabetes owing to its antioxidant action. It can also ameliorate the insulin resistance especially in primary human adipocytes.[25] Taxifolin (TAX) is another naturally occurring flavonoid having potential to reduce the oxidative stress which is induced by hyperglycemic states by the inhibition of recombinant aldose reductase and sorbitol.[26] TAX has antioxidant potential to protect the vascular tissues and heart against the oxidative stress and lipid peroxidation. TAX has significant role in reducing the apoptosis incidence.[27] It also has a significant role to inhibit the activity of α-amylase and ultimately decrease the rate of metabolism of carbohydrates which leads to lower the level of glucose in systemic circulation. TAX reduces the glucose level which is induced by osmotic stress via reduction of sorbitol and aldose reductase in human. Recently, it has proved that TAX protects the vascular tissues and heart by providing the protection against the lipid peroxidation and by reducing the apoptosis incidence.[9] Therefore, it is important that inhibitors of carbohydrate metabolizing enzymes may be one of the choices of therapeutic interventions for the treatment of postprandial hyperglycemia. Molecular docking is an efficient and highly accurate prediction strategy for the identification of the structures of protein–ligand complexes, which are helpful in computations for recognition of molecules especially for designing of drug molecule.[28] It considers all the factors including active site of receptors, small molecular structure, ligand binding, and determines the low-energy binding modes.[29] For the development of cost-effective and alternative anti-diabetic drugs, there is need to determine the routes to decrease the production of enzymes that are involved in the digestion of carbohydrates.[30]

The aim of current study was to investigate the in vitro characterization of RSV and TAX against carbohydrate metabolizing enzymes. Furthermore, we performed molecular docking in order to get the information about the molecular aspects of these compounds. In this study, we determined in vitro carbohydrates and incretin metabolic enzymatic activity of RSV and TAX to identify and confirm the glucoregulatory mode of action of these polyphenolic compounds. The inhibitory assays along with kinetic studies were performed for the evaluation of inhibitory potential and binding modes of RSV and TAX with α-amylase, α-glucosidase, and DPP-IV assay kits. We validated our hypothesis via molecular docking of RSV and TAX with these enzymes via standard inhibitors acarbose (ACB), miglitol (MGL), and diprotin A (DPT), respectively.

Materials and Methods

Materials Required

Resveratrol (CHEM-IMPEX INT'L INC), taxifolin (Sigma aldrich), acarbose (Carbosnyth,USA), diprotin (Sigma

aldrich), HPA assay kit (Product code: K-CERA, Megazyme brand), α-glucosidase assay kit (Product code: MAK123, Sigma aldrich), DPP-IV inhibitor screening assay kit (Product code: ab133081 Abcam), starch (Sigma aldrich) and all the other materials of analytical grade were used.

In vitro *Inhibitory Activity of Bioactive Compounds Against α-glucosidase*

The mixture of 17 μL of 5 mM pNPG (4, nitrophenyl α-D-glucopyranoside) and 5 μL of RSV and TAX solutions, with different concentrations (0, 10, 25, 50, 75, and 100 μ*M*), were incorporated into 96 well microplate. Afterwards, this mixture was incubated for 5 min at 37 °C. After performing incubation, 17 μL of .15 μg/mL GLU solution was put in each well microplate. Again, the mixture was incubated till the end of hydrolytic reaction. After 15 min, 100 μL of 200 mM solution of sodium carbonate was incorporated into each well microplate to block the proceeding of reaction. At the end, the absorbance was calculated at 405 nm by employing a microplate reader. The results of GLU activity were presented in IC_{50} as described previously.[31]

The method of linear regression equation was adopted to calculate the IC_{50} accompanying a graph showing the concentration of sample on *x*-axis while % inhibition on *y*-axis. By employing equation of linear regression, that is, $y = a + bx$, the values of IC_{50} were calculated

$$IC_{50} = \frac{50 - a}{b}$$

In vitro *Inhibitory Activity of Bioactive Compounds Against α-amylase*

Around 250 μL of bioactive compounds (RSV and TAX) of different concentrations (0, 10, 25, 50, 75, and 100 μg/mL), 2% (w/v) starch, and 250 μL of 1 U/mL HPA solution were mixed homogenously in test tube. The mixed solution was incubated at 20 °C for 3 min. After incubation, 500 μL of dinitro salicylic acid (colored reagent) was added in each well to stop the enzymatic reaction. Then mixture was put into boiled water and 250 μL of HPA1 U/mL was added immediately. The mixture was heated continuously for 15 min and then allowed to cool at room temperature. To make the total volume of solution up to 6000 μL, 4500 μL of distilled water was added into the solution and mixed well using a vortex mixer. The activity of HPA was calculated by measuring the absorbance at 540 nm via spectrophotometry. The absorbance of product was compared with blank solution. The % inhibition was calculated by using equation.[32] The data obtained from HPA activity was used for determination of % inhibition by using following equation

$$\% \text{ inhibition} = \frac{A_1 - A_2}{A_1} \times 100$$

where A1 is absorbance of blank and A2 is absorbance of sample. These results were processed in the form of graph and compared with % inhibition of ACB as positive control. The value of IC_{50} was calculated by following the same procedure as described above.

In vitro *Inhibitory Activity of Bioactive Compounds Against DPP-IV*

The *in vitro* gastrointestinal digestion model was established by following the instructions and protocols as described previously.[33] The inhibitory activity of bioactive compounds against DPP-IV in the existence of Gly-Pro-AMC with a concentration range of 0 to 60 μM was carried out by following the instructions of assay reagent kit's manufacturer as described previously and presented in terms of IC_{50}.[34]

Inhibitory Kinetics Study of Bioactive Compounds

The inhibitory actions of RSV and TAX against carbohydrate metabolizing were determined at 0.25 and 0.5 mg/mL, separately. Each sample of different concentrations was estimated in the existence of Gly-Pro-AMC with various concentrations (0–60 μM). The pattern of inhibition was determined by employing Lineweaver-Burk plot. The constant (K_i) which is known as inhibition constant was calculated with help of a graph showing a reciprocal relationship with initial luminescence and substrate.[35]

Computational Study and Molecular Docking of Bioactive Compounds

Structural preparation and docking studies. The co-crystal structure of carbohydrate metabolizing enzymes such as human α-amylase (HPA) and DPP-IV were obtained from data bank of RCB protein with entries such as 1HNY (HPA) and 4A5S (DPP-IV). For protein modeling, Phyre2 online server was used to develop the 3D structure of GLU.[36] The FASTA sequences having NCBI Accession no P07265 were obtained from uniprot.[37] The 3D-macromolecular structure with maximum Phyre2 confidence score was downloaded and carefully analyzed to avoid any stereo-chemical deformity. In order to predict the quality of Phyre2 generated protein structure, Psi/Phi Ramachandran plot was generated by submitting 3D-conformation of GLU into the PRO-CHECK webserver.[38] Furthermore, the ProSAweb web tool[39] was utilized to compute empirically derived Z-scores to countercheck the quality of generated structural model. Likewise, the co-crystalized structures of 1HNY and 4A5S were also carefully inspected by employing SYBYL-X 1.3 module to authenticate chemical accuracy.[40] Missing hydrogens were computationally added. The appropriate charges and atoms were employed as recommended by

AMBER7FF99 force field,[41] accompanied by a loss of energy by employing Powell algorithm[42] with .5 kcal/ (mol•Å) convergence gradient followed by 1000 cycles. The Figure 1 is showing the 3D-structures of bioactive ligands accompanying with standard inhibitors such as miglitol (MGL), acarbose (ACB), and diprotin (DPT) of carbohydrate metabolizing enzymes. The structures were built by using SKETCH module implemented in Sybyl-X1.3.[43] The energy optimization of generated 3D-conformations of TAX, RSV, ACB, MGL, and DPT was performed as suggested by Tripos force field with Gasteigere Huckel atomic charge. Finally, the compounds TAX, RSV, ACB, MGL, and DPT were docked with their particular targets by employing Surflex-Dock (flexible) SYBYL-X 1.3 module[43] molecular modeling software package to get insight into the binding modes of tested compounds bonded to HPA, GLU, and DPP-IV enzymes. Top twenty docking generated putative poses were saved for each inhibitor. SYBYL utilizes the Hammerhead scoring (*cScore*) function[40,44] to rank putative poses of ligands in their corresponding complexes. All settings for Surflex-Docking were kept same as mentioned in our study.[45]

Molecular dynamics simulation studies. The structural models of complexes of TAX and RSV bonded to HPA, GLU, and DPP-IV, as exhibited in Figure 1C, were processed by employing MD simulation strategy in order to inspect their structural behaviors. The MD-simulations were accomplished with the help of AMBER-16 software[46] along with

ff99SB force field.[47] Likewise, docking complexes of standard compounds as exhibited in Figure 1C bonded to their respective molecular targets (ACB-HPA, MGL-GLU, and DPT-DPP-IV) were also subjected to MD-simulation. Moreover, a comparison between binding free energies of TAX- and RSV-enzyme complexes with standard compounds, that is, ACB, MGL, and DPT-bonded systems were investigated by employing the approach of MM/PB(GB)SA.[48] All MD simulations and binding free energies (MM/PB(GB)SA) were computed with AMBER16 software package,[49] by employing same strategy as mentioned in our previous work.[9,45]

Statistical analysis. The results of *in vitro* study are expressed as mean ± SD (standard deviation) (n = 6) by using Graph pad prism. The results were statistically analyzed by employing One-Way ANOVA followed by a post hoc test known as Dunnett's test. The value of $P<.05$ was considered as significant.

Results

We measured the *in vitro* inhibitory activities of various concentrations of RSV and TAX against α-glucosidase, α-amylase, and DPP-IV. We also investigated the inhibitory activity of each concentration of RSV and TAX accompanying Gly-Pro-AMC (0–60 μM) in various concentrations and exhibited the *in vitro* % inhibition against carbohydrate metabolizing enzymes with IC_{50} values as shown in Table 1. Both bioactive compounds
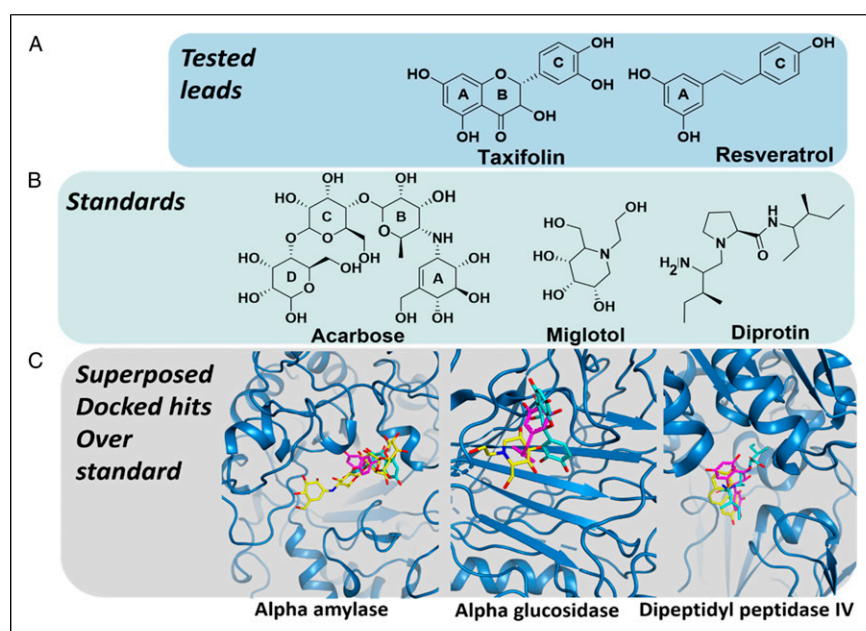
Figure 1. Chemical structures of selected ligands for molecular docking analysis. (A) Chemical structures of tested compounds taxifolin (TAX) and resveratrol (RSV). (B) 2D-structural representation of standard compounds acarbose (ACB), miglitol (MGL), and diprotin (DPT). (C) Supposed conformation of selected hits and standard compound in their corresponding molecular targets.

exhibited their inhibitory activity against DPP-IV more significantly as compared to that of their positive control.

In vitro *Inhibitory Activity of Bioactive Compounds Against α-glucosidase*

The *in vitro* inhibitory effect of bioactive compounds (RSV, TAX) on enzymatic activity of GLU was measured by using pNPG as substrate while acarbose used as positive control. Based on IC_{50} values, we affirmed that RSV and TAX has inhibitory effect on GLU with IC_{50} (47.93±5.21 μM and 45.86 ± 3.78 μM), respectively. But these compounds have weak inhibiting effect on GLU as compared to acarbose IC_{50} (4.6 ± 1.26 μM) as shown in Table 1.

In vitro *Inhibitory Activity of Bioactive Compounds Against α-amylase*

The in vitro inhibitory effect of RSV and TAX on enzymatic activity of HPA was measured by using starch as substrate while acarbose was used as positive control. RSV and TAX have IC_{50} value 32.23 ± .556 μM and 31.26 ± .556 μM, respectively, showing that higher significant effect in comparison to acarbose (IC_{50}: 77.88 ± .277 μM) as exhibited in Table 1. However, RSV and TAX have approximately same inhibitory effect on HPA enzyme.

In vitro *Inhibitory Activity of Bioactive Compounds Against DPP-IV*

The *in vitro* inhibitory activity of RSV and TAX on enzymatic activity of DPP-IV was investigated using diprotin A was used as positive control. The result was concluded based on IC_{50} values, RSV and TAX have strong inhibitory effect showing IC_{50} value (5.638 ± .0016 μM and 6.691 ± .004), respectively, in comparison to diprotin A (3.21 ± .021 μM).

Molecular Docking of Bioactive Compounds

The outcomes of *in vitro* studies demonstrate that TAX and RSV exhibit the remarkable binding affinity towards HPA, GLU, and DPP-IV enzymes as compared to their benchmark inhibitors;

ACR, MGL, and DPT, respectively. In order to compare the interaction pattern of tested compounds and the standard inhibitor of GLU, 3D structure of GLU was modeled followed by molecular docking studies as exhibited in figure 1B. The best phyre2 predicted structure of GLU according to Phyre2 confidence (93%) was selected for further processing. The findings of empirically derived Z-score and Ramachandran plot (Figure 2) further supported the reliability and accuracy of our modeled structure. The Ramachandran plot for GLU protein depicts that 99.2% of residues lie in the allowed region including 88.2% in most favored region. Furthermore, appreciable values of Z-score (−10.58) also suggest that the quality modeled structure is good enough to be used for docking analysis.

In this study, MD simulation studies were carried out to identify the variations in binding mode studied ligands in their complexes, which may explain the difference in the affinities of ligands towards target proteins. The top-ranked docking generated conformations according to cumulative score (cScore) were selected as shown in Table 2. The scores of TAX, ACB, and RSV for HPA were 7.82, 7.22, and 6.90, respectively, and these scores indicated that TAX had almost same affinity towards HPA as that of ACB. Although, RSV demonstrated slight less binding affinity among three HPA-bonded systems, the binding affinity still reflects that RSV is tightly bonded to HPA. In DPP-IV bonded system, TAX and RSV exhibited the significant affinity (cScore: 5.43 and 5.54, respectively) towards DPP-IV as compared to standard inhibitor such as DPT (cScore: 4.26). Both studied hits of bioactive compounds showed the decreased values of cScore in GLU-bonded systems as compared to GLU-MGL system. However, there was no significant variation between the Score of GLU-TAX and GLU-MGL suggesting the binding affinity of TAX towards GLU is comparable to that of GLU-MGL system. The docking scores accompanying a list of residues contributing H-bonding are summarized in Table 2. The top-ranking docking generated putative poses of studied hits were saved and viewed graphically in biopolymer module (SYBYL-X 1.3) in order to determine the possible variations in the interaction pattern of different ligands bonded to same molecular target as exhibited in Figure 3. Furthermore, the simple 2D receptor-ligand diagram showing the interaction of whole docking pose as exhibited in Figure 4 give more detailed insight into variations in the mode of ligand-receptor interactions.

Table 1. Inhibitory Activity of Bioactive Compounds Against GLU, HPA, and DPP-IV Enzymes.

Parameters	α-glucosidase	α-amylase	DPP-IV	DPP-IV
	IC_{50} (μM) ± SD	IC_{50} (μM) ± SD	IC_{50} (μM) ± SD	$K_i (\mu M)$
Positive control l (Diprotin A)	-	-	7.21 ± .021	7.32
Positive control l (Acarbose)	4.6 ± 1.26	77.88 ± .277	-	10.76
Resveratrol (RSV)	47.93 ± 5.21	32.23 ± .556	5.638 ± .0016	14.96
Taxifolin (TAX)	45.86 ± 3.78	31.26 ± .556	6.691 ± .004	12.31

Abbreviations: IC50; inhibitory concentration is measure at the half maximal, SD; standard deviation, K_i; inhibition constant.
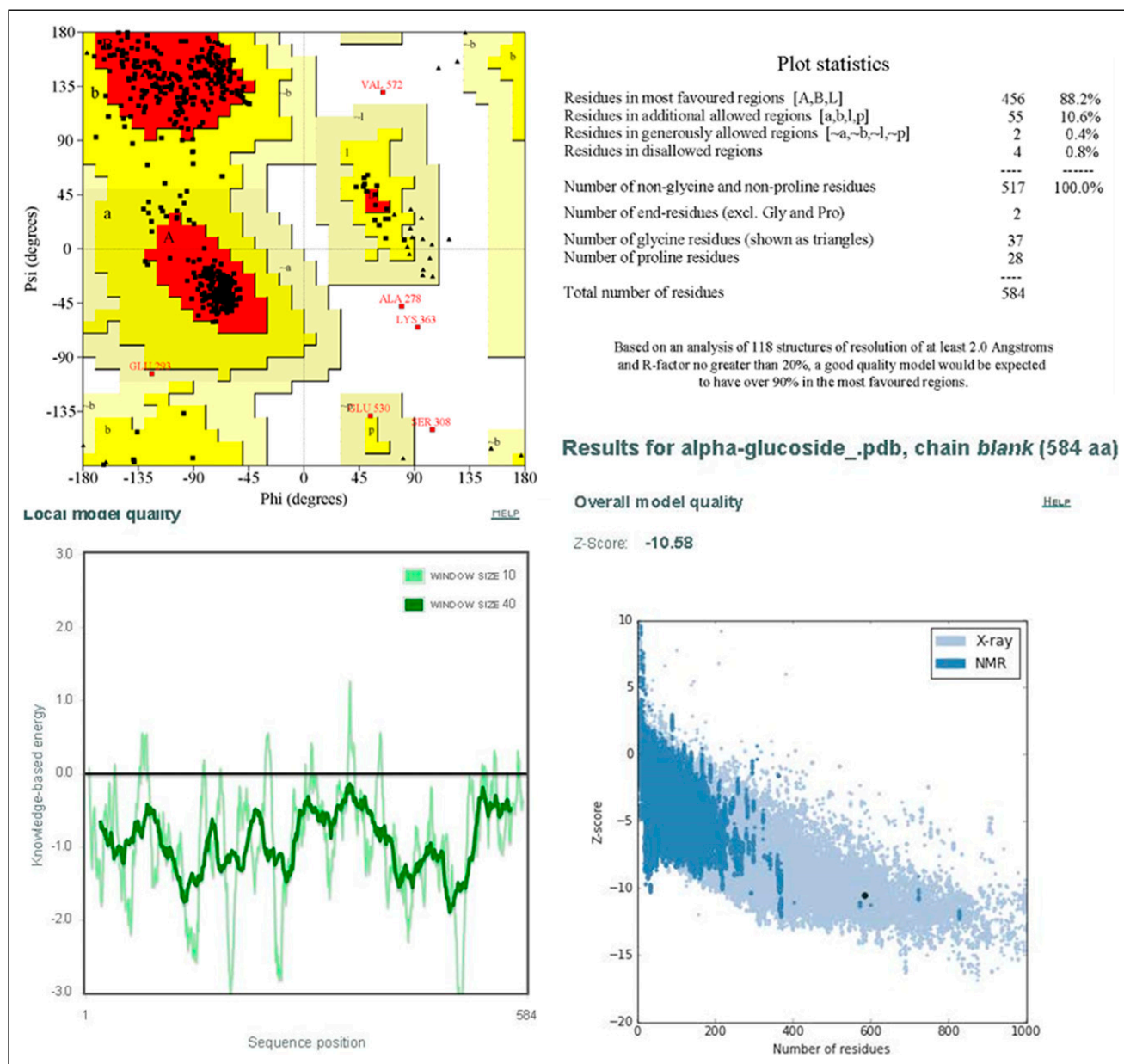
Figure 2. Ramachandran Plot analysis performed with PROCHECK online webserver and ProsWeb generated Z-score graph.

Molecular Dynamic Simulation Studies

All the 9 docking complexes; ACB-HPA, TAX-HPA, RSV-HPA, MGL-GLU, TAX-GLU, RSV-GLU, DPT-DPP-IV, TAX-DPP-4, and RSV-DPP-IV were subjected to MD simulations to identify the molecular interactions. All of nine complexes were post-processed with MD simulations for 30 ns and the RMSD (root-mean-square deviation) was computed during the entire simulation time to elucidate the stability of studied complexes in solution. As depicted in Figure 5, all complex systems retained their structural conformation intact and stable throughout the simulation period while the RMSD values remained below 2.5 Å for protein, pocket, or ligand.

Among all 3 complexes, the least RMSD was found to be displayed by TAX in HPA-TAX bonded system (Figure 5B), which confirms that the ligand TAX is tightly complexed with HPA. The highest value of docking scores also supports these findings as depicted in Figure 6, all the ligands remained intact in its complex form without any loss of key interactions.

MM/PB(GB)SA

Finally, a comprehensive analysis of computed binding free energies of TAX and RSV towards HPA, GLU, and DPP-IV

Table 2. Surflex Score of Docked Ligands; Taxifolin and Resveratrol for GLU, HPA, and DPP-IV Along With Their Corresponding Standard Molecules Acarbose, Miglitol, and Diprotin A.

| Protein	Ligands	CScore	Crash score	Polar score	G score	PMF score	D score	Chem score	Amino acid interaction
α-amylase	Acarbose	7.22	−3.27	6.36	−204.817	−10.715	−162.326	3.965	D300, E233, H201, K200
	Resveratrol	6.90	−1.11	4.98	−159.609	−16.661	−92.326	−17.170	R195, D197, D300, H299
	Taxifolin	7.82	−.94	4.14	−208.162	−42.372	−119.501	−13.290	Q63, E233, R199, D197, H299
α-glucosidase	Miglitol	4.95	−.95	6.40	−68.447	−31.476	−724.892	−7.277	D91, W126
	Resveratrol	4.17	−.60	4.01	−120.570	−7.402	−96.736	−10.412	R331, C127, W126, D91, I98, A93
	Taxifolin	4.74	−1.03	4.02	−88.053	2.091	−84.855	−10.702	P94, I98, R331, D91, W126, C127
DPP-IV	Diprotin	4.26	−1.14	2.67	−161.702	−37.837	−112.472	−11.725	Y547, E205, S630, H740, N710
	Resveratrol	5.54	−1.45	4.28	−105.239	24.386	−70.525	−18.476	Y547, R669, E206, V207, R358
	Taxifolin	5.43	−.89	6.01	−143.571	20.390	−66.641	−17.637	Y547, E206, R669
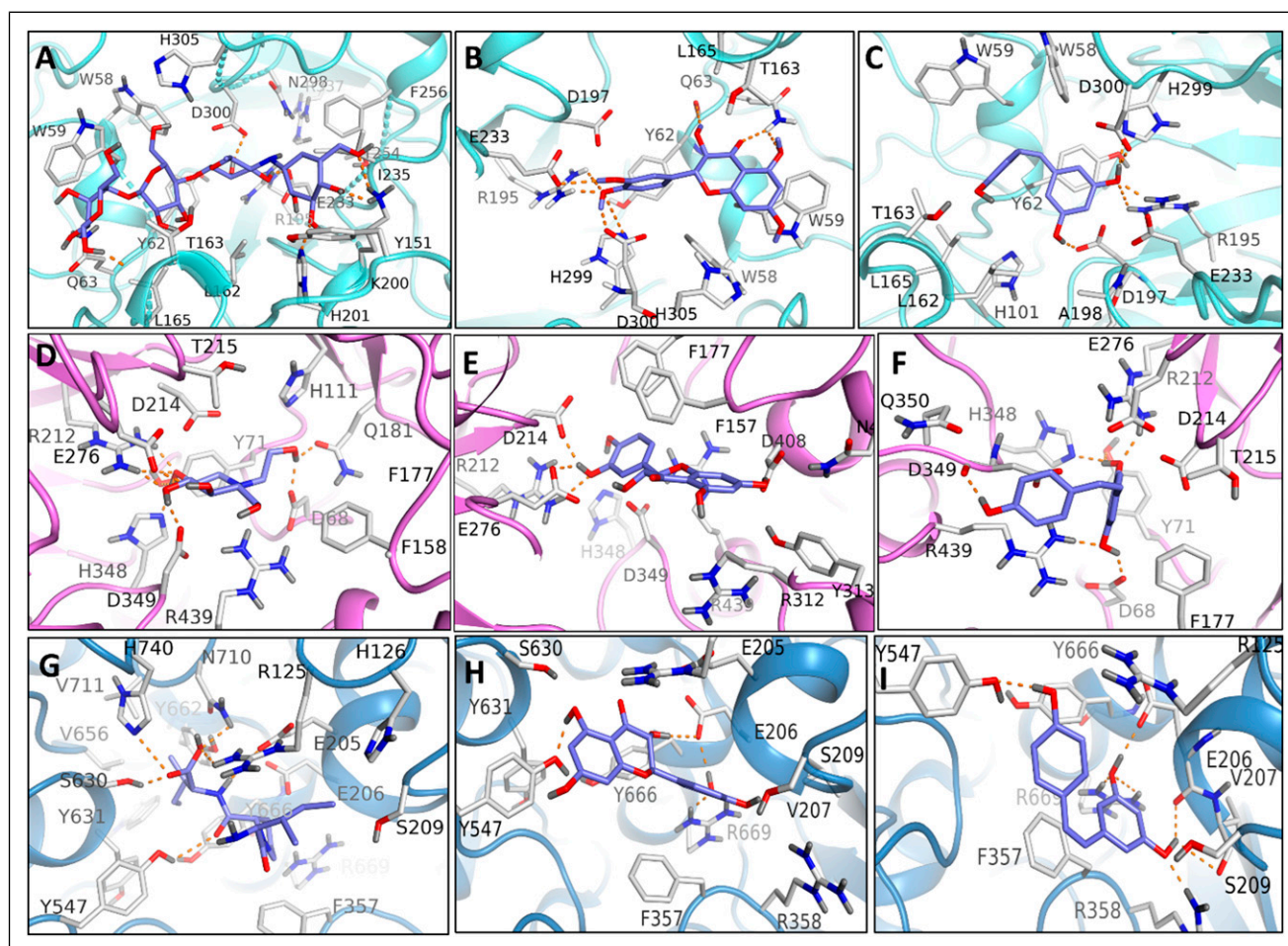
Figure 3. Docking generated complexes of enzymes; HPA, GLU, and DPP-IV bonded to their standard inhibitors and tested compounds: (A) ACB-HPA (B) TAX-HPA (C) RSV-HPA, (D) MGL-GLU (E) TAX-GLU (F) RSV-GLU (G) DPT-DPP-IV (H) TAX-DPP-IV (I) RSV-DPP-IV.
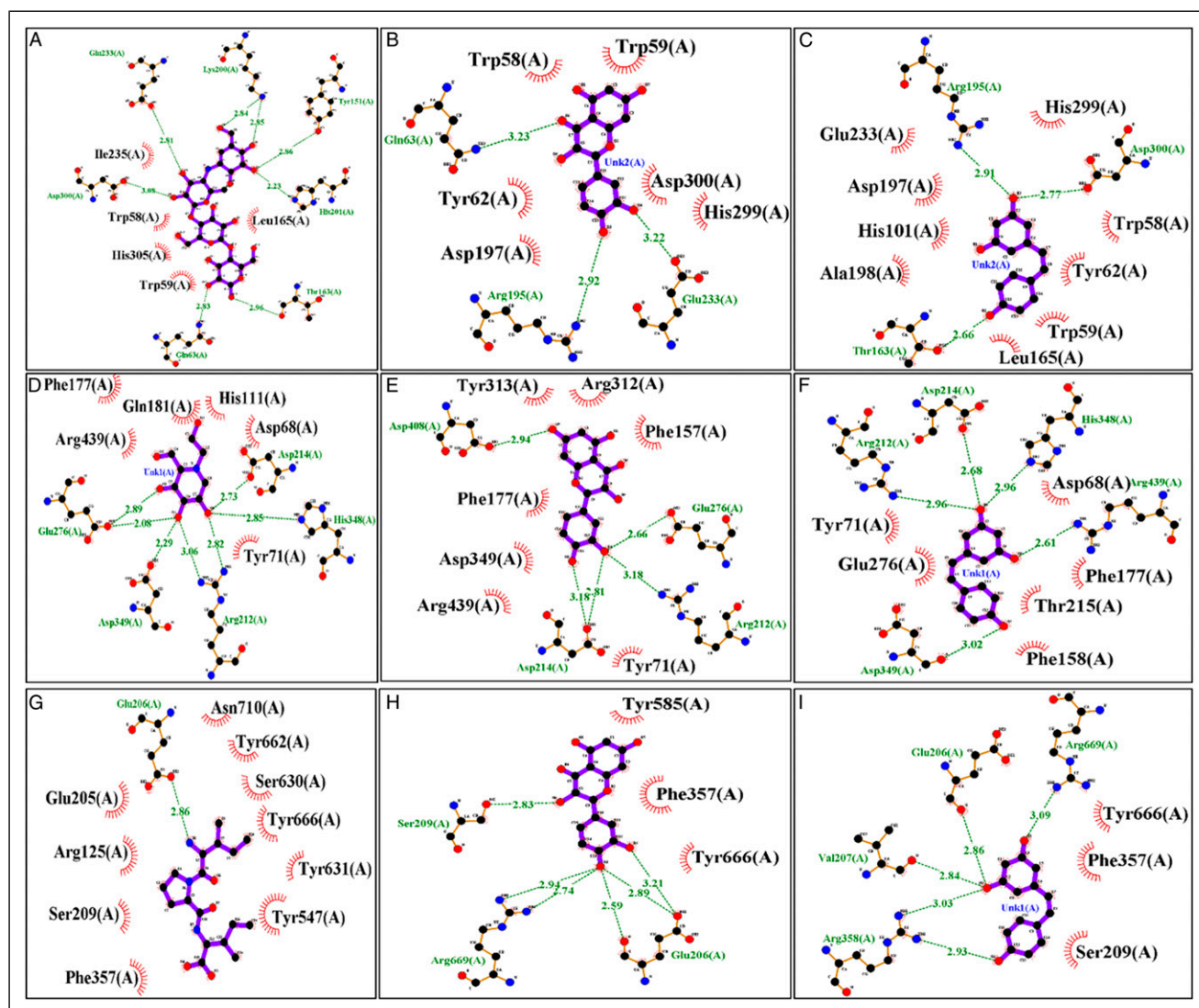
Figure 4. The diagram of 2D-ligand-protein interaction was retrieved in order to obtain best poses with ACB (A) and TAX (B) and RSV(C) against AML crystal structure. Ligands bonded to GLU enzyme are depicted in (D) MGL (E) TAX and (F) RSV. DPP-4 bonded complexes are (G) DPT (TAX) and (RSV). The H-bonding is represented via green and blue dotted arrows as H-bond donor/accepter pattern, respectively.

enzymes was conducted by applying MM/PB(GB)SA approach. The same approach using aforementioned protocols and parameters was utilized to measure the binding affinities of standard inhibitors; ACB, MLG, and DPT bonded to their respective molecular targets; HPA, GLU, and DPP-IV. The obtained values of binding free energy terms for standard-enzyme complexes and TAX- and RSV-enzyme complexes were graphically depicted to individually compare the binding affinities of ligand-protein complexes with each other as exhibited in Figure 7. The calculation of binding free energy $\Delta G_{pred(GB)}$ on the basis of MM/PB(GB)SA exhibits that both compounds TAX and RSV (−29.85 kcal/mol; −18.92 kcal/mol, respectively) are entrapped within HPA-binding cleft as compared to standard compound (−11.25 kcal/mol). Since, TAX demonstrates the highest variations in the values of

$\Delta G_{pred(GB)}$ for HPA as compared to ACB and RSV, providing an indication that the TAX has highest selectivity towards HPA as compared to other compounds (Figure 7A). Likewise, the calculation of binding free energies on the basis of MM/PBSA also exhibits the variations in pattern of binding affinities, providing an indication that TAX and RSV show equal potential towards HPA ($\Delta G_{pre(PB)}$ −19.68 kcal/mol; −19.84 kcal/mol, respectively) than ACB ($\Delta G_{pre(PB)}$ −8.93 kcal·mol^{-1}). Similarly, in GLU-bonded systems RSV and TAX demonstrates slightly better binding affinities ($\Delta G_{pre(PB)}$ −34.60 and −31.32 kcal·mol^{-1}) for GLU than the corresponding value ($\Delta G_{pre(PB)}$ −29 kcal·mol^{-1}) of MGL-GLU system (Figure 7B). Among DPP-IV-ligand systems, again compound TAX displayed even superior binding affinities ($\Delta G_{pre(PB)}$ −8.93 kcal·mol^{-1}) than the standard compound DPP
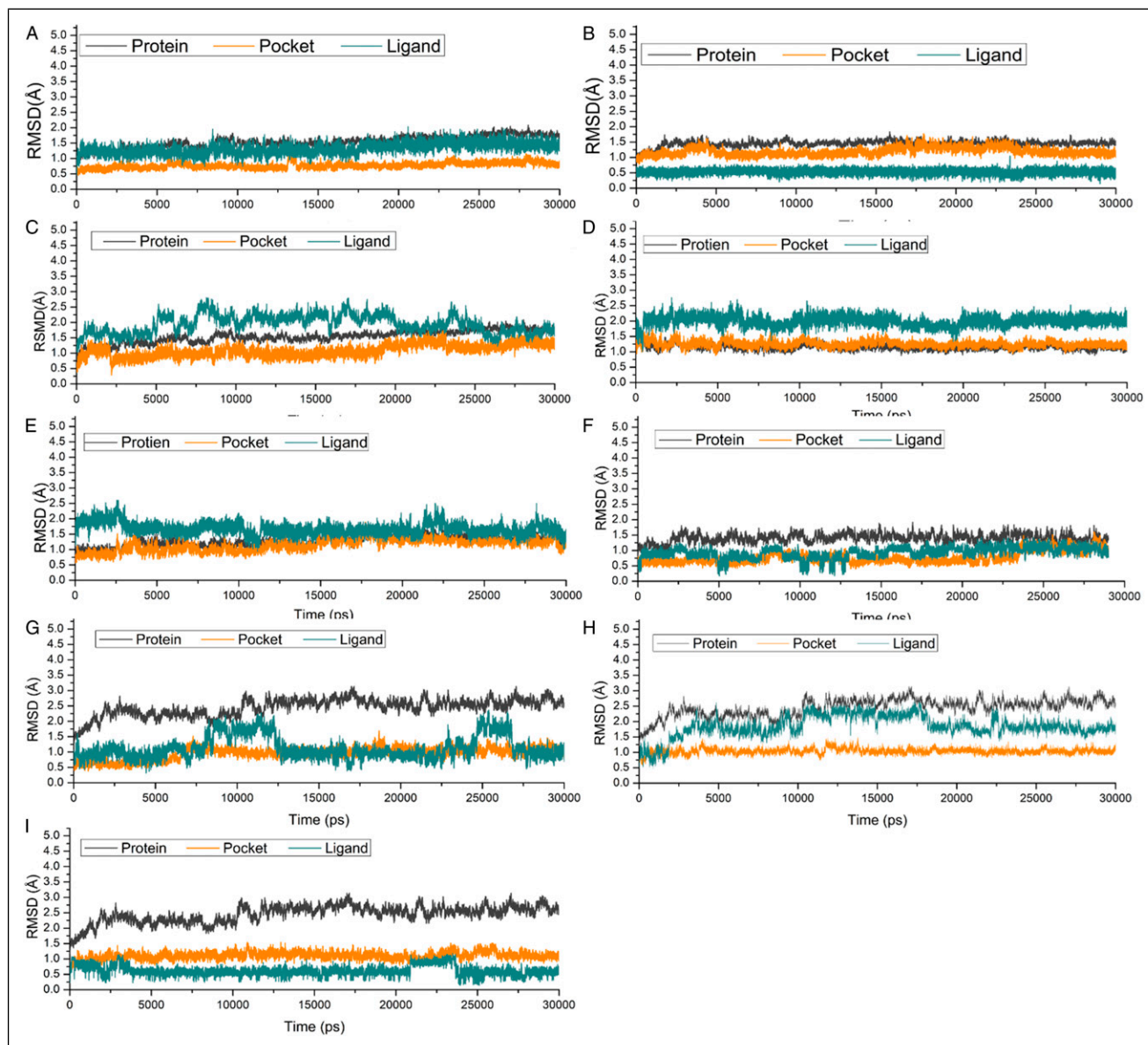
Figure 5. RMSDs of Cα atoms of the protein, backbone atoms of binding pocket (within 6.5 Å), and the heavy atoms in the ligand for: (A) ACB-HPA (B) TAX-HPA (C) RSV-HPA, (D) MGL-GLU (E) TAX-GLU (F) RSV-GLU (G) DPT-DPP-IV (H) TAX-DPP-IV (I) RSV-DPP-IV.

($\Delta G_{pre(PB)}$ −40.33 kcal·mol^{-1}). Although, compound RSV shares least binding affinity among studied DPP-IV-bonded systems as exhibited in Figure 7C, the difference in binding affinities is not too high indicating that RSV is also tightly bonded to DPP-IV.

Discussion

HPA is involved in the digestion of carbohydrates. It breaks down the α-(1,4)-glycosidic bonds of oligosaccharides during the formation of bolus and swallowing of food.[50] The inhibition of HPA has significant role in suppressing the postprandial hyperglycemia which in turn slows down the carbohydrate digestion and reduces the absorption of glucose into the blood stream. Similarly, the inhibitors of GLU enzyme are obtained from various plant-based sources that suppress the hydrolysis of oligosaccharides. As a result, the release of α-glucose is diminished along with retardation in the digestion of carbohydrates and glucose absorption in the small intestine. This mechanism has significant role in maintaining the postprandial hyperglycemia and considered as novel therapeutic approach for the stabilization of blood glucose status in diabetic patients.[51] DPP-IV inhibitors are currently used as antihyperglycemic agents that block the enzymatic activity of DPP-IV which is a serine protease present in the endothelial layer of blood vessels, kidneys, and gastrointestinal tract. They deactivate the insulinotropic polypeptide, incretin, and GLP-1, which are considered
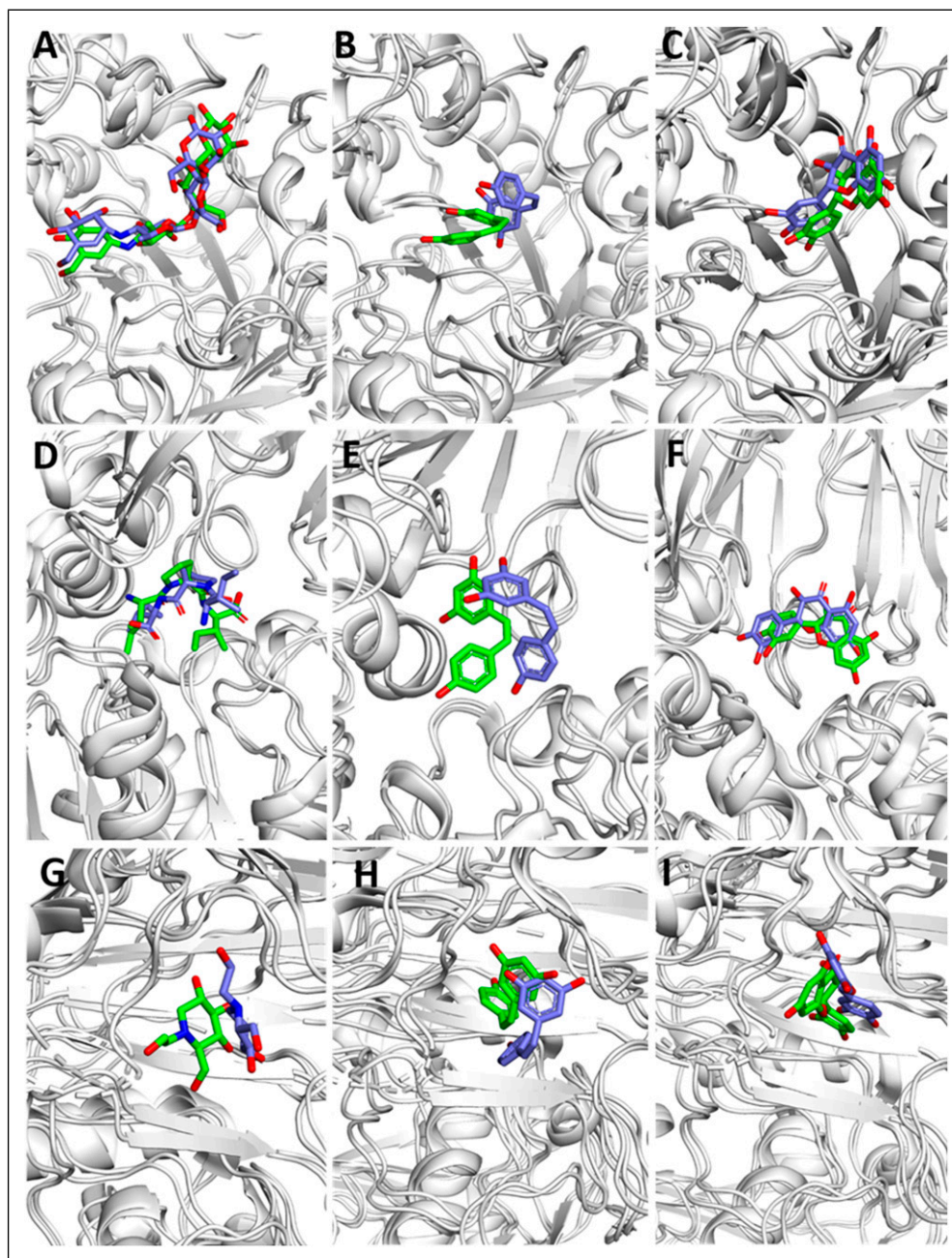
Figure 6. Structure comparison between initial (green) and representative snapshots from MD (slate) of: (A) ACB-AML (B) TAX-AML (C) RSV-AML, (D) MGL-GLU (E) TAX-GLU (F) RSV-GLU (G) DPT-DPP-IV (H) TAX-DPP-IV (I) RSV-DPP-IV.

essential for the secretion of insulin from pancreatic β-cells and suppression of pancreatic glucagon secretion.[52,53] Commercially available GLU inhibitors are non-selective drugs that also inhibit the pancreatic HPA leading to serious gastrointestinal side effects which is a major drawback of GLU inhibitors.[54] Therefore, there is an utmost need to discover and develop new drugs having strong GLU inhibitory activity but mild potential to inhibit pancreatic HPA activity.[55] Many polyphenols have ideal structural attributes including hydrophobic nature, flexible backbone, and several hydrogen bond donor and acceptor. By keeping in view these attributes, we selected two polyphenols, RSV and TAX for evaluation of percentage inhibitory activity against carbohydrate (GLU and HPA) and GLP-1 metabolizing for RSV and TAX, separately. Many methods are available for the enzymatic assays[56] but we employed in vitro and in silico approaches for initial screening and comparison among selected bioactive compounds.
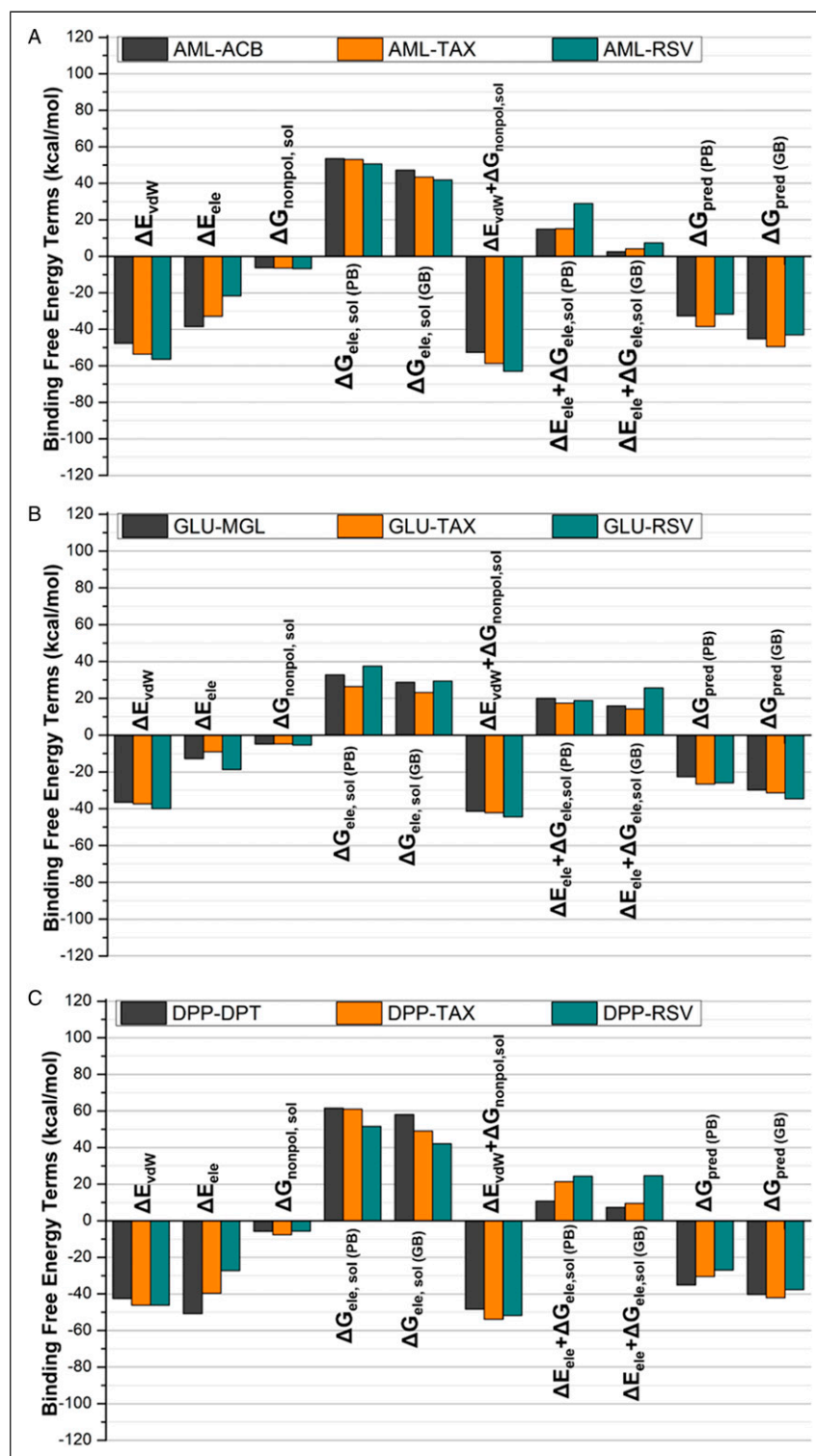
Figure 7. Comparison among free energy terms of: (A) HPA linked to ACB, TAX, and RSV; (B) GLU linked to MGL, TAX and RSV; (C) DPP-IV linked to DPT, RAX, RSV.

The *In vitro* activity of RSV and TAX has affirmed that both bioactive compounds have significant inhibitory potential as shown in Table 1. The % inhibition at various concentrations of RSV and TAX exhibited that inhibition percentage depends upon the concentration. RSV and TAX have high HPA inhibitory activity as compared to that of positive control (acarbose). Both bioactive compounds can exhibit high inhibitory activity than the acarbose even in smaller

concentration. The results of our experiments with respect to GLU are inconsistent with reported study.[57] While, TAX inhibits GLU activity in a competitive manner.[58] The literature showed that dietary polyphenols including RSV have GLU inhibitory activity and used as supplementation for the treatment of diabetes as anti-diabetic agents.[59] Our study confirmed that RSV and TAX have the potential to inhibit the enzymatic activity of GLU that may lead to lower the post-prandial hyperglycemia and potentially inhibit the intestinal GLU activity. Inhibition of GLU activity is prominent mechanism in contributing the anti-diabetic activity. We also determined the *in vitro* inhibitory activity of RSV and TAX against HPA as exhibited in Table 1. HPA cleaves the glycosidic bond in starch, but RSV and TAX inhibit the activity of α-amylase. Due to this mechanism of action, starch cannot form the disaccharides in body. HPA facilitates GLU for conversion of disaccharides into monosaccharides and maintains the level of glucose.[60] Our study confirmed that RSV and TAX inhibit GLU and HPA enzymes and help to regulate the metabolism of carbohydrates and hyperglycemic status. Our results are in consistent with already published data showing that RSV has potential to inhibit GLU,[57] as well as TAX also has GLU inhibitory activity as previously reported.[61] Our results regarding the inhibition of HPA by RSV and TAX are supported by published data.[9,62] RSV and TAX can inhibit DPP-IV to regulate the glucose homeostasis. TAX inhibits DPP-IV with less activity with high IC_{50} value as compared to RSV. Our results regarding DPP-IV inhibitory effects by RSV and TAX are in accordance with published data.[63,64] The docking technique is utilized to investigate the interactions between small molecule and protein at atomic level to predict the binding behavior of small molecules toward protein along with elucidation of fundamental biochemical processes. Two main steps are involved in docking: to predict the conformation, position, and orientation of ligand and estimate the binding affinity of ligand.[65] The prediction of electronic characteristics which replicated our experimental results was measured by top ranked docked poses of HPA-TAX and -RSV complexes. The MD simulations have strong impact in the field of molecular biology as well as drug discovery. These simulations are helpful to analyze and understand the behavior of biomolecules and proteins at atomic level with fine temporal resolution.[66]

The best docking conformations were saved for each compound and investigated to explore the differences in ligand-protein interactions patterns accounting for difference in binding affinities of ligands to its target protein as exhibited in Figure 3. As shown in Figure 1C and 3A-C, all three ligands adopt similar pattern of interaction within the binding cavity of HPA to develop H-bond contacts with surrounding residues. In HPA-ligand bonded systems, W58, W59, T62, Q63, H101, L162, L165, R195, D197, A198, G233, I235, F256, H299, D300, H305, G306, and A307 are the key amino-acids constituting the active site of HPA. The best docked model of ACB-HPA complex, as exhibited in Figure 3A, reveals that

the ACB predominantly occupies the binding site of HPA to establish eight H-bond contacts with nearby residues such as Q63, Y153, T163, K200, H201, E233, H299, and D300. Interestingly, E233 and D300 are more crucial as these are involved in the hydrolysis of carbohydrates. These residues have been investigated in order to detect their interactions with ethyl caffeate and myricetin,[67] which authenticates the rationality of docking results. In order to elucidate the interaction pattern of TAX and RSV with HPA, the top ranked docked poses of HPA-TAX and -RSV complexes were also evaluated critically exhibited in Figure 3B and C. The results of molecular docking exhibits that various residues involving in HPA-ACB complexation also contribute to form TAX and RSV-HPA complex system. However, unlike ACB-HPA system, TAX establishes only three H-bond interactions Q63, R195, and E233 of HPA is unable to interact with TAX. Similarly, RSV also establishes a set of triple H-bond interactions with residues T163, R195, and D300.

However, it was not surprising as TAX and RSV exhibit smaller structural dimensions as compared to ACB. Both rings of TAX designated as A and B extend in a reverse way in cleft (ligand binding) of HPA, where they can also establish π-π interaction with Tyr62 and Trp59 as exhibited in Figure 2B. However, this type of interaction was not observed in acarbose based RSV and HPA system because acarbose lack aromatic ring as shown in Figure 1 and 2B. Despite of greater number of H bond interaction in ACB-HPA system, the better binding affinity of TAX in is mainly attributed by the other non-bonding interactions. Thus, the fluctuations in interaction pattern of ligand-receptor can increase the HPA inhibitory potential of TAX as compared to RSV and ACB. The top-ranked docking generated conformations for GLU-bonded systems (GLU-MGL, TAX and RSV) were saved and visualized to explore the variations in binding modes of ligands bonded to GLU. Docking results demonstrated that in GLU-bonded system, compounds TAX and RSV are positioned in such a way to establish the similar mode of interaction as that observed in MGL-GLU complex (Figure 3D-F). As shown in Figure 3, GLU-ligand bonded systems are the main residues that predominantly surround the ligand binding cavity. Encouragingly, previous study has also reported the same binding cavity as the preferred ligand binding site for GLU inhibitors.[68] As depicted in Figure 3D, the benchmark inhibitor of GLU (MGL) establishes several H-bonds with closely situated amino acid residues R212, D214, Q276, D349 and H348. Similarly, TAX also remained settled deep inside the active site of GLU, where it may form at least five H-bond interactions with residues E276, D408, R212, and D214 which reflect the fact that H-bond interactions in TAX-GLU system are relatively stronger than that of corresponding interaction of MGL-GLU complex. Likewise, the compound RSV develop a network of five H-bond interactions with residues H348, R212, D214, D349, and R349 with average distance of 3.0 Å. These results support the higher binding affinity of RSV towards GLU than TAX and MLG. However, all the ligands

demonstrated the appreciable binding tendency towards GLU. Since, the residues R212 and D214 have been identified to be involved in making common H-bond interaction in all ligand-GLU bonded systems; these may be regarded as the key contributor in ligand-GLU complex formation. In DPP-IV-bonded systems, DPT, TAX and RSV can establish a network of H-bond interactions (Figure 3G-I). A conserved H-bond interaction between E206 of DPP-4 and compounds DPT, TAX and RSV has been observed which highlights E206 as crucial residue for DPP-IV-ligand complex formation. Interestingly, E206 has previously been reported to make ionic interaction in DPP-IV-ligand complexes. In addition, a pair of conserve H-bonds can be seen between R669 of DPP-IV and tested leads TAX and RSV. Since, more than five H-bond interactions were found in TAX- and RSV-DPP-4 systems while only one H-bond interaction was observed in DPT-DPP-IV system, these variations in pattern of interactions may explain the superior binding affinity of TAX and RSV over DPT.

MM/PB(GB)SA provides us an opportunity to decompose total binding free energies into independent components. The MM/PB(GB)SA binding energies were resolved into energy components behaving independent and revealing deriving forces that are responsible for variation in affinities of ligands towards GLU, HPA and DPP-4. The vdW and energy associated with solvation energy ($\Delta E vdW + \Delta G nonpol,sol$) increase either from $\pi - \pi$ stacking, $\sigma - \pi$ stacking, or vdW contacts play a very essential role in binding of TAX with HPA (-18.52 kcal•mol-1). The $\Delta E vdW$ component for ACB-bonded system is still slightly higher than (-45.19 kcal•mol-1) than the corresponding value in RSV-bonded system. In addition, $\Delta G ele$ contribution in ACB-HPA bonded complex is highest among all three systems, suggesting that higher binding affinity of ACB than RSV was the consequence of $\Delta G ele$ as exhibited in Figure 7A and Table 3. Despite of similar $\Delta G ele$ contribution in GLU-bonded systems, the smaller $\Delta G pred$ (GB) values for TAX and MGL bonded systems than GLU-RSV are the consequence of higher

Table 3. Comparison Between Binding Free Energies of Standard Compound Acarbose ACB With TAX and RSV Bond with Alpha-Amylase.

Protein-inhibitor	HPA-ACR	HAP-TAX	HAP-RSV
ΔE_{vdW}	-47.64	-53.62	-56.33
ΔE_{ele}	-38.53	-32.86	-21.65
$\Delta G_{nonpol, sol}$	-6.25	-6.38	-6.70
$\Delta G_{ele, sol (PB)}$	53.48	53.03	50.62
$\Delta G_{ele, sol (GB)}$	47.23	43.39	41.81
$\Delta E_{vdW}+\Delta G_{nonpol,sol}$	-52.67	-58.64	-63.03
$\Delta E_{ele}+\Delta G_{ele,sol (PB)}$	14.95	15.14	28.97
$\Delta E_{ele}+\Delta G_{ele,sol (GB)}$	2.45	4.14	7.32
$\Delta G_{pred (PB)}$	-32.69	-38.49	-31.66
$\Delta G_{pred (GB)}$	-45.19	-49.48	-43.05

Table 4. Comparison Between Binding Free Energies of Miglitol (MGL) With Tested Compounds TAX and RSV Bond With GLU.

Protein-Inhibitor	GLU-MGL	GLU-TAX	GLU-RSV
ΔE_{vdW}	-36.51	-37.37	-39.99
ΔE_{ele}	-12.76	-9.01	-18.71
$\Delta G_{nonpol, sol}$	-4.88	-4.76	-5.43
$\Delta G_{ele, sol (PB)}$	32.77	26.39	37.49
$\Delta G_{ele, sol (GB)}$	28.66	23.18	29.31
$\Delta E_{vdW}+\Delta G_{nonpol,sol}$	41.39	42.13	44.43
$\Delta E_{ele}+\Delta G_{ele,sol (PB)}$	20.01	17.38	$18,78$
$\Delta E_{ele}+\Delta G_{ele,sol (GB)}$	15.90	14.17	25.65
$\Delta G_{pred (PB)}$	-22.66	-26.58	-25.97
$\Delta G_{pred (GB)}$	-29.81	-31.32	-34.60

Table 5. Comparison Between Binding Free Energies of Diprotin (DPT) With TAX and RSV Bond With DPP-IV.

Protein-inhibitor	DPP-DPT	DPP-TAX	DPP-RSV
ΔE_{vdW}	-42.51	-46.16	-46.18
ΔE_{ele}	-50.86	-39.62	-27.27
$\Delta G_{nonpol, sol}$	-5.79	-7.68	-5.66
$\Delta G_{ele, sol (PB)}$	61.61	60.98	51.58
$\Delta G_{ele, sol (GB)}$	58.02	49.11	42.10
$\Delta E_{vdW}+\Delta G_{nonpol,sol}$	48.30	53.84	51.84
$\Delta E_{ele}+\Delta G_{ele,sol (PB)}$	10.75	21.36	24.31
$\Delta E_{ele}+\Delta G_{ele,sol (GB)}$	7.34	9.49	24.57
$\Delta G_{pred (PB)}$	-35.07	-30.50	-26.91
$\Delta G_{pred (GB)}$	-40.33	-42.06	-37.66

favorable $\Delta E vdW + \Delta G nonpol,sol$ and energies as exhibited in Figure 7B and Table 4 in TAX-GLU complex. Likewise, $\Delta E vdW$ energy component has found to be the key driving force in DPP-4-ligand complex formation. In addition, favorable $\Delta E vdW + \Delta G nonpol,sol$ contribution is the main driving force for the higher binding affinity of TAX-bonded system as exhibited in Figure 7C and Table 5.

Conclusion

This study has evaluated the therapeutic potential of bioactive compounds (RSV and TAX) for the mitigation of DM by investigating the inhibitory impact of bioactive compounds on HPA, GLU, and DPP-IV activity through *in vitro* analysis. We also confirmed the enzyme binding potential of tested bioactive compounds by employing various computational tools and MD simulations. The results of this study confirmed that these bioactive compounds are potent inhibitor of HPA, GLU, and DPP-IV as compared to standards and exhibited high potential to prevent postprandial hyperglycemia. Resveratrol and taxifolin have the potential to inhibit the activity of α-amylase, α-glucosidase

as result reduce the metabolism of carbohydrates . Our results also suggest that both bioactive compounds significantly inhibit the DPP-IV enzymatic activity for glycemic control. Keeping aside the significant results found from *in vitro* experiments, the MD simulations also revealed the high binding affinities of RSV and TAX with HPA as compared to their other corresponding complex systems. This study will provide full insight to use bioactive compounds for management of diabetes mellitus irrespective of already available anti-diabetic drugs to avoid side effects.

Declaration of Conflicting Interests

Funding

ORCID iDs

Kanwal Irshad https://orcid.org/0000-0003-1903-4502

Muhammad Sajid Hamid Akash https://orcid.org/0000-0002-9446-5233

References

1. Campbell RK. Fate of the beta-cell in the pathophysiology of type 2 diabetes. *J Am Pharm Assoc*. 2009;49(suppl 1):S10-S15.

2. World Health Organization. Global status report on non-communicable diseases. 2010. Available from. https://www.who.int/nmh/publications/ncd_report2010/en/https://www.who.int/nmh/publications/ncd_report2010/en/.

3. Petrie JR, Pearson ER, Sutherland C. Implications of genome wide association studies for the understanding of type 2 diabetes pathophysiology. *Biochem Pharmacol*. 2011;81:471-477.

4. Chaudhury A, Duvoor C, Reddy Dendi VS, Kraleti S, Chada A, Ravilla R, et al. Clinical review of antidiabetic drugs: Implications for type 2 diabetes mellitus management. *Front Endocrinol*. 2017; 8:6.

5. Ross SA, Ekoé JM. Incretin agents in type 2 diabetes. *Can Fam Physician*. 2010;56:639-648.

6. de Souza PM, de Oliveira Magalhães P. Application of microbial α-amylase in industry - A review. *Braz J Microbiol*. 2010;41: 850-861.

7. Navarro DMDL, Abelilla JJ, Stein HH. Structures and characteristics of carbohydrates in diets fed to pigs: a review. *J Anim Sci Biotechnol*. 2019;10:39.

8. Rehman K, Ashraf A, Azam F, Akash MSH. Effect of food azo-dye tartrazine on physiological functions of pancreas and glucose homeostasis. *Turkish J Biochem*. 2019;44:197-206.

9. Rehman K, Chohan TA, Waheed I, Gilani Z, Akash MSH. Taxifolin prevents postprandial hyperglycemia by regulating the activity of α-amylase: Evidence from an in vivo and in silico studies. *J Cell Biochem*. 2019;120:425-438.

10. Fujisawa T, Ikegami H, Inoue K, Kawabata Y, Ogihara T. Effect of two alpha-glucosidase inhibitors, voglibose and acarbose, on postprandial hyperglycemia correlates with subjective abdominal symptoms. *Metabolism*. 2005;54:387-390.

11. Rehman K, Rashid U, Jabeen K, Akash MSH. Morin attenuates *L*-arginine induced acute pancreatitis in rats by downregulating myeloperoxidase and lipid peroxidation. *Asian Pac J Trop Biomed*. 2021;11:148-154.

12. Drucker DJ. Incretin-based therapy and the quest for sustained improvements in β-cell health. *Diabetes Care*. 2011;34: 2133-2135.

13. Nauck MA. Incretin-based therapies for type 2 diabetes mellitus: properties, functions, and clinical implications. *Am J Med*. 2011; 124:S3-S18.

14. Holst JJ, Vilsbøll T, Deacon CF. The incretin system and its role in type 2 diabetes mellitus. *Mol Cell Endocrinol*. 2009;297: 127-136.

15. Deacon CF. Circulation and degradation of GIP and GLP-1. *Horm Metab Res*. 2004;36:761-765.

16. Deacon CF, Nauck MA, Meier J, Hücking K, Holst JJ. Degradation of endogenous and exogenous gastric inhibitory polypeptide in healthy and in type 2 diabetic subjects as revealed using a new assay for the intact peptide. *J Clin Endocrinol Metab*. 2000;85:3575-3581.

17. Rehman K, Ali MB, Akash MSH. Genistein enhances the secretion of glucagon-like peptide-1 (GLP-1) via downregulation of inflammatory responses. *Biomed Pharmacother*. 2019;112:108670.

18. Semighini EP, Resende JA, de Andrade P, Morais PA, Carvalho I, Taft CA, et al. Using computer-aided drug design and medicinal chemistry strategies in the fight against diabetes. *J Biomol Struct Dyn*. 2011;28:787-796.

19. Rasouli H, Farzaei MH, Khodarahmi R. Polyphenols and their benefits: A review. *Int J Food Prop*. 2017;20:1700-1741.

20. Chan WH. Effect of resveratrol on high glucose-induced stress in human leukemia K562 cells. *J Cell Biochem*. 2005;94: 1267-1279.

21. Rehman K, Akash MSH. Mechanism of Generation of Oxidative Stress and Pathophysiology of Type 2 Diabetes Mellitus: How Are They Interlinked?. *J Cell Biochem*. 2017;118: 3577-3585.

22. Nanjan MJ, Betz J. Resveratrol for the Management of Diabetes and its Downstream Pathologies. *Eur Endocrinol*. 2014;10: 31-35.

23. Brasnyó P, Molnár GA, Mohás M, Markó L, Laczy B, Cseh J, et al. Resveratrol improves insulin sensitivity, reduces oxidative stress and activates the Akt pathway in type 2 diabetic patients. *Br J Nutr*. 2011;106:383-389.

24. Bhatt JK, Thomas S, Nanjan MJ. Resveratrol supplementation improves glycemic control in type 2 diabetes mellitus. *Nutr Res*. 2012;32:537-541.

25. Chuang CC, Martinez K, Xie G, Kennedy A, Bumrungpert A, Overman A, et al. Quercetin is equally or more effective than resveratrol in attenuating tumor necrosis factor-{alpha}-mediated inflammation and insulin resistance in primary human adipocytes. *Am J Clin Nutr*. 2010;92:1511-1521.

26. Haraguchi H, Ohmi I, Fukuda A, Tamura Y, Mizutani K, Tanaka O, et al. Inhibition of aldose reductase and sorbitol accumulation by astilbin and taxifolin dihydroflavonols in Engelhardtia chrysolepis. *Biosci Biotechnol Biochem*. 1997;61:651-654.

27. Vladimirov YA, Proskurnina EV, Demin EM, Matveeva NS, Lubitskiy OB, Novikov AA, et al. Dihydroquercetin (taxifolin) and other flavonoids as inhibitors of free radical formation at key stages of apoptosis. *Biochemistry (Mosc)*. 2009;74:301-307.

28. Wang R, Lu Y, Wang S. Comparative evaluation of 11 scoring functions for molecular docking. *J Med Chem*. 2003;46:2287-2303.

29. Ewing TJ, Makino S, Skillman AG, Kuntz ID. DOCK 4.0: search strategies for automated molecular docking of flexible molecule databases. *J Comput Aided Mol Des*. 2001;15:411-428.

30. Kumar B, Gupta SK, Nag TC, Srivastava S, Saxena R, Jha KA, et al. Retinal neuroprotective effects of quercetin in streptozotocin-induced diabetic rats. *Exp Eye Res*. 2014;125:193-202.

31. Dewi RT, Iskandar YM, Hanafi M, Kardono LB, Angelina M, Dewijanti ID, et al. Inhibitory effect of koji Aspergillus terreus on alpha-glucosidase activity and postprandial hyperglycemia. *Pak J Biol Sci*. 2007;10:3131-3135.

32. Ali H, Houghton PJ, Soumyanath A. alpha-Amylase inhibitory activity of some Malaysian plants used to treat diabetes; with particular reference to Phyllanthus amarus. *J Ethnopharmacol*. 2006;107:449-455.

33. Oomen AG, Hack A, Minekus M, Zeijdner E, Cornelis C, Schoeters G, et al. Comparison of five in vitro digestion models to study the bioaccessibility of soil contaminants. *Environ Sci Technol*. 2002;36:3326-3334.

34. Velarde-Salcedo AJ, Barrera-Pacheco A, Lara-González S, Montero-Morán GM, Díaz-Gois A, González de Mejia E, et al. In vitro inhibition of dipeptidyl peptidase IV by peptides derived from the hydrolysis of amaranth (Amaranthus hypochondriacus L.) proteins. *Food Chem*. 2013;136:758-764.

35. Fan J, Johnson MH, Lila MA, Yousef G, de Mejia EG. Berry and Citrus Phenolic Compounds Inhibit Dipeptidyl Peptidase IV: Implications in Diabetes Management. *Evid base Compl Alternative Med*. 2013;2013:479505.

36. Kelley LA, Mezulis S, Yates CM, Wass MN, Sternberg MJ. The Phyre2 web portal for protein modeling, prediction and analysis. *Nat Protoc*. 2015;10:845.

37. UniProt Consortium. UniProt: a hub for protein information. *Nucleic Acids Res*. 2014;43:D204-D212.

38. Laskowski RA, MacArthur MW, Moss DS, Thornton JM. PROCHECK: a program to check the stereochemical quality of protein structures. *J Appl Crystallogr*. 1993;26:283-291.

39. Wiederstein M, Sippl MJ. ProSA-web: interactive web service for the recognition of errors in three-dimensional structures of proteins. *Nucleic Acids Res*. 2007;35:W407-W410.

40. Jain AN. Surflex: fully automatic flexible molecular docking using a molecular similarity-based search engine. *J Med Chem*. 2003;46:499-511.

41. Case DA, Darden T, Cheatham TE III, Simmerling C, Wang J, Duke RE, et al. *AMBER 9*. San Francisco: University of California; 2006:45.

42. Powell MJ. *A Fast Algorithm for Nonlinearly Constrained Optimization calculationsNumerical Analysis*. Springer; 1978: 144-157.

43. SYBYL-X 1.3. *Molecular Modeling Software*. South Hanley Road, St. Louis, MO 631444, USA: Tripose Inc.; 1699. Available from: https://sybyl-x.software.informer.com/1.3/.

44. Jain AN. Scoring noncovalent protein-ligand interactions: a continuous differentiable function tuned to compute binding affinities. *J Comput Aided Mol Des*. 1996;10:427-440.

45. Chohan TA, Chen J-J, Qian H-Y, Pan Y-L, Chen J-Z. Molecular modeling studies to characterize N-phenylpyrimidin-2-amine selectivity for CDK2 and CDK4 through 3D-QSAR and molecular dynamics simulations. *Mol Biosyst*. 2016;12:1250-1268.

46. Case D, Darden T, Cheatham TE III, Simmerling C, Wang J, Duke R, et al. *AMBER 12*. San Francisco: University of California; 2012:1.

47. Duan Y, Wu C, Chowdhury S, Lee MC, Xiong G, Zhang W, et al. A point-charge force field for molecular mechanics simulations of proteins based on condensed-phase quantum mechanical calculations. *J Comput Chem*. 2003;24:1999-2012.

48. Gohlke H, Case DA. Converging free energy estimates: MM-PB (GB) SA studies on the protein–protein complex Ras–Raf. *J Comput Chem*. 2004;25:238-250.

49. Case D, Betz R, Cerutti D, Cheatham T, Darden T, Duke R. *AMBER16*. San Francisco; 2016.

50. Alam F, Islam MA, Kamal MA, Gan SH. Updates on Managing Type 2 Diabetes Mellitus with Natural Products: Towards Antidiabetic Drug Development. *Curr Med Chem*. 2018;25: 5395-5431.

51. Hossain U, Das AK, Ghosh S, Sil PC. An overview on the role of bioactive α-glucosidase inhibitors in ameliorating diabetic complications. *Food Chem Toxicol*. 2020;145:111738.

52. Kim BR, Kim HY, Choi I, Kim JB, Jin CH, Han AR. DPP-IV Inhibitory Potentials of Flavonol Glycosides Isolated from the Seeds of Lens culinaris: In Vitro and Molecular Docking Analyses. *Molecules*. 2018;23.

53. Holst JJ. The incretin system in healthy humans: The role of GIP and GLP-1. *Metabolism*. 2019;96:46-55.

54. Yousefi A, Yousefi R, Panahi F, Sarikhani S, Zolghadr AR, Bahaoddini A, et al. Novel curcumin-based pyrano[2,3-d] pyrimidine anti-oxidant inhibitors for α-amylase and α-glucosidase: Implications for their pleiotropic effects against diabetes complications. *Int J Biol Macromol*. 2015;78:46-55.

55. Mehrabi M, Esmaeili S, Ezati M, Abassi M, Rasouli H, Nazari D, et al. Antioxidant and glycohydrolase inhibitory behavior of curcumin-based compounds: Synthesis and evaluation of antidiabetic properties in vitro. *Bioorg Chem*. 2021;110:104720.

56. Sales PM, Souza PM, Simeoni LA, Silveira D. α-Amylase inhibitors: a review of raw material and isolated compounds from plant source. *J Pharm Pharm Sci*. 2012;15:141-183.

57. Hu J, Zhang B, Du L, Chen J, Lu Q. Resveratrol ameliorates cadmium induced renal oxidative damage and inflammation. *Int J Clin Exp Med*. 2017;10:7563-7572.

58. Liu J, Wang X, Geng S, Liu B, Liang G. Inhibitory mechanism of taxifolin against α-glucosidase based on spectrofluorimetry and molecular docking. *Nat Prod Commun*. 2017;12: 1934578X1701201116.

59. Zhang J, Rimando A, Mizuno C, Mathews S. α-glucosidase inhibitory effect of resveratrol and piceatannol. *J Nutr Biochem*. 2017;47.

60. Elya B, Handayani R, Sauriasari R, Hasyyati US, Permana IT, Permatasari YI. Antidiabetic activity and phytochemical screening of extracts from Indonesian plants by inhibition of alpha amylase, alpha glucosidase and dipeptidyl peptidase IV. *Pak J Biol Sci*. 2015;18:279.

61. Liu J, Wang X, Geng S, Liu B, Liang G. Inhibitory mechanism of taxifolin against α-glucosidase based on spectrofluorimetry and molecular docking. *Natural Product Communications*. 2017;12:1934578X1701201116.

62. Mattio LM, Marengo M, Parravicini C, Eberini I, Dallavalle S, Bonomi F, et al. Inhibition of Pancreatic α-amylase by Resveratrol Derivatives: Biological Activity and Molecular Modelling Evidence for Cooperativity between Viniferin Enantiomers. *Molecules*. 2019;24.

63. Fan J, Johnson MH, Lila MA, Yousef G, de Mejia EG. Berry and citrus phenolic compounds inhibit dipeptidyl peptidase IV: Implications in diabetes management. *Evid Based Complement Alternat Med*. 2013;2013:479505.

64. Proena C, Freitas M, Ribeiro D, Tom SM, Arajo AN, Silva AMS, et al. The dipeptidyl peptidase-4 inhibitory effect of flavonoids is hindered in protein rich environments. *Food Funct*. 2019;10:5718-5731.

65. McConkey BJ, Sobolev V, Edelman M. The performance of current methods in ligand–protein docking. *Curr Sci*. 2002: 845-856.

66. Hollingsworth SA, Dror RO. Molecular Dynamics Simulation for All. *Neuron*. 2018;99:1129-1143.

67. Williams LK, Li C, Withers SG, Brayer GD. Order and disorder: differential structural impacts of myricetin and ethyl caffeate on human amylase, an antidiabetic target. *J Med Chem*. 2012;55: 10177-10186.

68. Amin S, Ullah B, Ali M, Rauf A, Khan H, Uriarte E, et al. Potent in vitro α-glucosidase inhibition of secondary metabolites derived from *Dryopteris cycadina*. *Molecules*. 2019; 24:427.